Inland navigation channel model for fault detection and control: Application to the Cuinchy-Fontinettes reach

Eric Duviella,
Laurent Bako
and Moamar Sayed-Mouchaweh
Univ Lille Nord de France, F-59000 Lille, France
MinesDouai, IA, F-59500 Douai, France
Cor. Author: eric.duviella@mines-douai.fr

Joaquim Blesa,
Yolanda Bolea
and Vivenç Puig
Automatic Control Department
Universitat Politecnica de Catalunya
Pla de Palau, 18 , 08003 Barcelona, Spain

Karine Chuquet
VNF - Service de la navigation
du Nord Pas-de-Calais
37 rue du Plat, 59034 Lille Cedex, France

***Abstract*—Inland navigation networks offer an alternative to land transport with economic and environmental benefits, and direct access to urban and industrial centers. Promoting the navigation transport requires the modernization of the network management, in particular the control of navigation levels and the improvement of the network safety. To reach these aims, modeling methods of the inland navigation networks have to be proposed. These networks are large scale distributed systems characterized by non-linearities, time-delays and generally no significant slope. A modeling method of a navigation channel based on identification method is proposed in this paper. It is applied on the Cuinchy-Fontinettes reach located in the north of France.**

I. Introduction

In a context of global climate change, the alternative offered by the transport using inland navigation networks appears to be increasingly interesting. It provides economic and environmental benefits [14], [13] by offering access to the continent's urban and industrial centers, and allowing an efficient, quieter, and safer transport of goods [2]. To promote this type of transport, inland navigation networks in the north of Europe will have to be able to accommodate large broad gauge boats with the increasing of the navigation schedules. This requires the implementation of sensors and actuators, control and supervision architectures based on Information and Communication Technology (ICT); the principal aims being the improvement of the seaworthiness requirements of the navigation channels. In particular, the water level of the channels has to be close to the Normal Navigation Level (NNL). This aim requires the development and tuning of new control algorithms considering stronger constraints. Indeed, automatic control provide more accuracy and reliability than manual control. Moreover, sensor or actuator faults can lead to serious dysfunctions that can impact navigation, infrastructures, and water resources. Thus, Fault Detection and Isolation (FDI) techniques also have to be developped and tuned. The proposition of control and FDI algorithms requires a generic modeling approach of the inland navigation channels which allow to catch the particular wave phenomenas characterising the dynamics of these systems.

Inland navigation networks are composed of several reaches separated by locks. Generally, they are supplied by several inputs and can supply other hydraulic systems. These reaches are large open-channel systems with no significant slope and characterized by multi-inputs-multi-ouputs (MIMO) and time-delays. They can be modeled by the Saint-Venant Partial Differential Equations [3] whose resolution involves numerical approaches according to discretization scheme. These numerical approaches are rather complex to handle in the control or FDI strategy design. On the other hand, the modeling techniques based on the simplification and linearization of the Saint-Venant equations such as in [9], might not be applicable to MIMO systems and they can not reflect the wave phenomenas. In [1], a control algorithm based on Model Predictive Control (MPC) is proposed to model a navigation reach with the aim to compensate or to reduce the waves impacting the reach. But the proposed model is only dedicated for control algorithm design. An alternative consists in proposing modeling approaches based on system identification techniques. Due to the importance of the transfer-delays, it is easier to have an *a priori* knowledge of them or to use a preliminary estimation technique according to the measurements on the system. Thus, this approach consists in a gray-box modeling.

Gray box modeling is a popular approach for modeling real systems, combining both black box and white box methodologies. Black box modeling is a method, which uses no knowledge of the physical system, but is based on experimental data only. The exact opposite is white box modeling, where all necessary information about the system is available, therefore the model can be constructed directly from prior knowledge. Gray

box modeling has the advantage of using both physical a priori knowledge of the system for model structure development, and parameter estimation from available experimental data. That is, gray box modeling of systems involves constructing a model structure based on physical knowledge of the system and model identification using estimation methods. Gray box modeling is an increasingly popular approach for studying hydrological, physiological, aero-spatial, environmental pollution and chemical (among others) systems where the process is known in some way [15].

In this paper, a gray-box modeling approach for MIMO time-delay open-channel systems is proposed. It is based on identification techniques according to measurement data. The Cuinchy-Fontinettes Reach (CFR) which is located in the north of France is modeled according to this approach. The waves phenomena occurs when the locks of the CFR are operated. They cause waves of more than ten centimeters along the channel. The proposed model can be used for FDI or control techniques. The structure of the paper is the following: Section II is dedicated to the proposition of the gray box modeling approach for inland navigation network. In Section III, the CFR is described and the application of the gray box modeling approach is presented. The effectiveness of the proposed modeling approach is compared to a model based on Saint-Venant equations [12] in Section IV.

II. Inland navigation networks modeling

Inland navigation networks are used essentially for navigation tasks. They are composed of navigation reaches, generally with no significant slope, interconnected by locks and gates. To assure the navigation, the level of these reaches must be controlled to be close to the Normal Navigation Level (NNL). This aim becomes critical due to new constraints for the accommodation of large broad gauge boats with the increasing of the navigation schedules, in a global change context. In addition, the locks and gates of the navigation reaches which are operated to allow the crossing of ships may cause wave phenomena along the reach. Generally, these waves are not significant, but sometimes, due to the dimension of the locks, the amplitude of the wave exceeds several tens of centimeters. Thus, new control algorithms have to be designed and tuned. Moreover, Fault Detection and Isolation (FDI) techniques must also be proposed to improve the efficiency of the control algorithms by minimizing the impacts of sensors and actuators faults. To design control and FDI algorithms, the proposition of modeling approaches of navigation reaches is necessary.

A navigation reach is an open-channel system characterized by large dimensions, and nonlinear dynamics with varying delays. By considering the operating point corresponding to the NNL, the dynamic of a reach can be modeled by a linear state-space model. State-space models are selected because they are suitable for the design of control or FDI algorithms for MIMO systems.

The state variables are chosen as the n_x measured levels on the system, *i.e.* $L_i(k)$. The input variables of the state-space model correspond to the n_u input/output discharges $Q_l(k)$

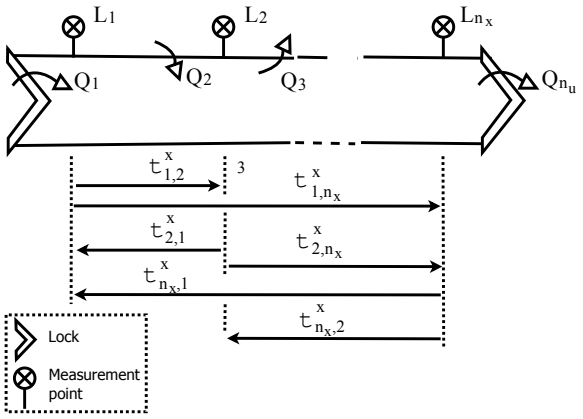

Figure 1. Time delays $\tau^x_{i,j}$ between each measurement points.

(*see* Figure 1). The output variables correspond directly to the state variables. Finally, time delay matrices τ^x and τ^u are considered for each state and input variables of the state space model to take into account the transfer delays of the reach. This modeling approach allows to catch the wave phenomena by considering the influence among water levels. The wave phenomena are only caused by the inputs and outputs of the reach.

$$\begin{cases} x_{k+1} &= A\overline{x}_{k|\tau^x} + B\overline{u}_{k|\tau^u} \\ y_k &= Cx_k \end{cases} \tag{1}$$

where matrices $A \in \mathbb{R}^{n_x \times n_x.n_x}$, $B \in \mathbb{R}^{n_x \times n_u.n_x}$ and $C \in \mathbb{R}^{n_x \times n_x}$ are the state, input and output matrices, respectively. At each time k, the vector $\overline{u}_{k|\tau^u_i} \in \mathbb{R}^{n_u.n_x}$ representing the input variable is defined according to the delay matrix τ^u, the vector $\overline{x}_{k|\tau^x} \in \mathbb{R}^{n_x.n_x}$ representing the state variable according to the delay matrix τ^x. The matrices $\tau^x \in \mathbb{N}^{n_x \times n_x}$ and $\tau^u \in \mathbb{N}^{n_u \times n_x}$ gather the time delays between each measurement point (*see* Figure 1), and between each measurement point and each input and output of the system, respectively. For example, the value of $\tau^x_{i,j} \in \mathbb{N}$ is the time delay between the measurement points L_i and L_j.

$$\tau^x = \begin{bmatrix} \tau^x_{1,1} & \tau^x_{1,2} & \cdots & \tau^x_{1,n_x} \\ \tau^x_{2,1} & \tau^x_{2,2} & \cdots & \tau^x_{2,n_x} \\ \vdots & \vdots & \ddots & \vdots \\ \tau^x_{n_x,1} & \tau^x_{n_x,2} & \cdots & \tau^x_{n_x,n_x} \end{bmatrix} \tag{2}$$

The time delays $\tau^x_{i,j}$ are equal to 1 for $i = j$. The time delay matrices τ^x and τ^u are supposed to be known and constant. The vector $y_k \in \mathbb{R}^{n_x}$ represents the output variable of the system.

The elements of the matrices τ^x and τ^u can be obtained *a priori* by the correlation method (data-based procedure) or by the physical knowledge of the system. Consider two points along the canal, separated by a distance D: upstream and downstream points. According to [8], the theoretical value of the upstream time delay between these two points is evaluated

by computing the integral:

$$\tau_{dw} = \int_0^D \frac{dl}{c(l) + v(l)} \tag{3}$$

with $c(l)$ and $v(l)$ representing the celerity and the velocity respectively.

This corresponds to the minimum time required for a perturbation to travel from the upstream point to the downstream point. Analogously, the upstream time delay τ_{du} can be evaluated by:

$$\tau_{up} = \int_0^D \frac{dl}{c(l) - v(l)} \tag{4}$$

and corresponds to the maximum time required for a perturbation to travel from the upstream point to the downstream point. In both cases, we recover the classical value in the uniform case when v and c are constant: $\tau_{dw} = \frac{D}{c+v}$ and $\tau_{up} = \frac{D}{c-v}$, with $c = \sqrt{g\frac{S}{b}}$ and $v = \frac{Q}{S}$. The wet aeras S and the cross section b are chosen constant as the mean values, g is the gravity and Q is the average flow of the canal.

The vector x_k in (1) is:

$$x_k = [L_1(k)\ L_2(k)\ \cdots\ L_{n_x}(k)]^T \tag{5}$$

Thus, the vector $\overline{x}_{k|\tau^x}$ is built according to the matrix τ^x such as:

$$\begin{aligned}\overline{x}_{k|\tau^x} = [&L_1(k-\tau^x_{1,1})\ L_2(k-\tau^x_{1,2})\ \cdots\ L_{n_x}(k-\tau^x_{1,n_x})\\ &L_1(k-\tau^x_{2,1})\ L_2(k-\tau^x_{2,2})\ \cdots\ L_{n_x}(k-\tau^x_{2,n_x})\\ &\cdots\ L_{n_x}(k-\tau^x_{n_x,n_x})]^T\end{aligned} \tag{6}$$

The vector $\overline{u}_{k|\tau^u}$ is built according to the matrix τ^u similarly as relation (6):

$$\begin{aligned}\overline{u}_{k|\tau^u} = [&Q_1(k-\tau^u_{1,1})\ Q_2(k-\tau^u_{1,2})\ \cdots\ Q_{n_u}(k-\tau^u_{1,n_u})\\ &Q_1(k-\tau^u_{2,1})\ Q_2(k-\tau^u_{2,2})\ \cdots\ Q_{n_u}(k-\tau^u_{2,n_u})\\ &\cdots\ Q_{n_u}(k-\tau^u_{n_x,n_u})]^T\end{aligned} \tag{7}$$

The state, input and ouput matrices are defined as:

$$A = \begin{bmatrix} a_1^1 & a_2^1 & \cdots & a_{n_x}^1 & 0 & 0 & \cdots & 0 & \cdots & 0 \\ 0 & 0 & \cdots & 0 & a_1^2 & a_2^2 & \cdots & a_{n_x}^2 & \cdots & 0 \\ \vdots & \vdots & \ddots & \vdots & \vdots & \vdots & \ddots & \vdots & \ddots & \vdots \\ 0 & 0 & \cdots & 0 & 0 & 0 & \cdots & 0 & \cdots & a_{n_x}^{n_x} \end{bmatrix} \tag{8}$$

$$B = \begin{bmatrix} b_1^1 & b_2^1 & \cdots & b_{n_u}^1 & 0 & 0 & \cdots & 0 & \cdots & 0 \\ 0 & 0 & \cdots & 0 & b_1^2 & b_2^2 & \cdots & b_{n_u}^2 & \cdots & 0 \\ \vdots & \vdots & \ddots & \vdots & \vdots & \vdots & \ddots & \vdots & \ddots & \vdots \\ 0 & 0 & \cdots & 0 & 0 & 0 & \cdots & 0 & \cdots & b_{n_u}^{n_x} \end{bmatrix} \tag{9}$$

The matrix C is equal to the identity matrix of order n_x.

After the structure of the state-space model has been defined, the objective is to identify the matrices A and B. Model (1) can be rewritten as:

$$x_{k+1} \quad = \quad M\ \Phi_k \tag{10}$$

with $M = [A\ B]$ and $\Phi_k = [\overline{x}_{k|\tau^x}\ \overline{u}_{k|\tau^u}]^T$.

Then, the matrix M has to be determined according to an identification approach using available measured data. The data correspond to N samples of the discharges Q_i and levels L_i measured on a time interval. Based on relation (10), the matrix M is expressed in the following way:

$$M \quad = \quad X\ \overline{\Phi}^T\ (\overline{\Phi}\ \overline{\Phi}^T)^{-1} \tag{11}$$

with $X = [x_{T+1}\ \cdots\ x_N]$, $\overline{\Phi} = [\overline{\Phi}_T\ \cdots\ \overline{\Phi}_{N-1}]$, and $T = \max(\tau^x)+1$; $\max(\tau^x)$ being the maximum entry of the matrix τ^x(*see* relation (2)).

Considering the characteristics of the matrices A and B, and the size of X and $\overline{\Phi}$, it is easier to identify separatly each line of M, before rebuilding the global matrices A and B. The zeros of matrices A and B are not considered during the identification step. It is based on the principle that each state variable can be expressed such as the first state variable:

$$\begin{aligned}L_1(k+1) = &\ a_1^1\ L_1(k-\tau^x_{1,1}) + a_2^1\ L_2(k-\tau^x_{1,2}) + \cdots\\ &+a^1_{n_x}\ L_{n_x}(k-\tau^x_{1,n_x}) + b_1^1\ Q_1(k-\tau^u_{1,1})\\ &+b_2^1\ Q_2(k-\tau^u_{1,2}) + \cdots + b^1_{n_u}\ Q_{n_u}(k-\tau^u_{1,n_u})\end{aligned} \tag{12}$$

Using this particular structure of the state space model, the dynamics of a real navigation reach can be identified. The Cuinchy-Fontinettes reach is presented in the next section.

III. Cuincy-Fontinettes reach

A. Presentation

The Cuinchy-Fontinettes navigation reach (CFR) is part of the broad gauge river network of North of France. It is located between the upstream lock of Cuinchy at the East of the town Bethune and the downstream lock of Fontinettes at the Southwest of the town Saint-Omer (*see* Figure 2). The first part of the channel, *i.e.* $28.7\ km$ from Cuinchy to Aire-sur-la-Lys, is called "canal d'Aire" and has been built in 1820. The second part of the channel, *i.e.* $13.6\ km$ from Aire-sur-la-Lys to Saint-Omer, is called "canal de Neuffossé" and has been built in the eleventh century. The channel is entirely artificial with a bottom equal to $52\ m$ in average and no significant slope. Considering the navigation flow, the water runs off from Cuinchy to Fontinettes.

The CFR is managed by VNF (Voies Navigables de France) whose role is to maintain the level of the channel at $NNL = 4.26\ m$. To reach this aim, three points of the CFR must be controlled: the first is the Cuinchy lock and gate, the second is the Fontinettes lock and the third is the gate called "Porte de Garde" at Aire-sur-la-Lys. The control of Cuinchy and Fontinettes locks is constrained by the navigation demand. The size of the lock at Fontinettes is $13\ m$ high whereas the lock at Cuinchy is only $2\ m$ high. The operation of the Fontinettes lock causes a wave phenomena which impact the CFR during more than 2 hours with a maximum amplitude which exceeds $13\ cm$. A first control approach is proposed in [1] to limit the impact of this wave. In addition, the sensors and actuators of the CFR are, as every electronic device, subject to faults due to the weather and the environment. These sensors can

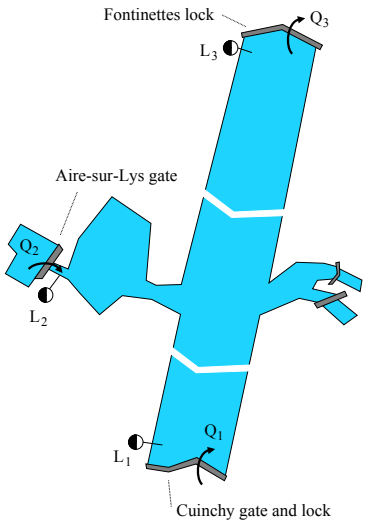

Figure 2. Scheme of the Cuinchy-Fontinettes navigation reach.

break down or be impacted over time. Several types of errors on sensors can occur. A bad setting of the sensors can lead to constant errors. This type of faults is particularly considered in [7] by focusing the FDI algorithm on the undershot/overshot gate: "Porte de Garde" at Aire-sur-la-Lys. To improve these contributions, a mode global model of the CFR has to be proposed. The state-space model presented in the last section is used to achieve this aim.

B. Gray-box modeling

The CFR is a MIMO system with three inputs, Q_1 for Cuinchy, Q_2 for Aire-sur-la-Lys, and Q_3 for Fontinettes, *i.e.* $n_u = 3$. The levels of the CFR are measured on three points; L_1 at Cuinchy, L_2 at Aire-sur-la-lys and L_3 at Fontinettes, *i.e.* $n_x = 3$. The time-delays are determined according to relations (3) and (4), with the wet aeras $S = 52 \times 4.26\ m^2$ (bottom $\times$ level of the water), and the maximum discharge $Q = 7.6\ m^3/s$ which is evaluated according to the Fontinettes lock operation. The matrices $\tau^x = \tau^u$ are given in minutes:

$$\tau^x = \begin{bmatrix} 1 & 74 & 109 \\ 75 & 1 & 35 \\ 110 & 36 & 1 \end{bmatrix} \tag{13}$$

The vector x_k is:

$$x_k = [L_1(k)\ L_2(k)\ L_3(k)]^T \tag{14}$$

and the vector $\overline{x}_{k|\tau^x}$ is given by:

$$\begin{aligned} \overline{x}_{k|\tau^x} = [&L_1(k-\tau^x_{1,1})\ L_2(k-\tau^x_{1,2})\ L_3(k-\tau^x_{1,3}) \\ &L_1(k-\tau^x_{2,1})\ L_2(k-\tau^x_{2,2})\ L_3(k-\tau^x_{2,3}) \\ &L_1(k-\tau^x_{3,1})\ L_2(k-\tau^x_{3,2})\ L_3(k-\tau^x_{3,3})]^T \end{aligned} \tag{15}$$

The vector $\overline{u}_{k|\tau^u}$ is:

$$\begin{aligned} \overline{u}_{k|\tau^u} = [&Q_1(k-\tau^u_{1,1})\ Q_2(k-\tau^u_{1,2})\ Q_3(k-\tau^u_{1,3}) \\ &Q_1(k-\tau^u_{2,1})\ Q_2(k-\tau^u_{2,2})\ Q_3(k-\tau^u_{2,3}) \\ &Q_1(k-\tau^u_{3,1})\ Q_2(k-\tau^u_{3,2})\ Q_3(k-\tau^u_{3,3})]^T \end{aligned} \tag{16}$$

The output matrix is equal to:

$$C = I_3 \tag{17}$$

The modeling approach consists in identifying the coefficients of the state and input matrices defined as:

$$A = \begin{bmatrix} a_1^1 & a_2^1 & a_3^1 & 0 & 0 & 0 & 0 & 0 & 0 \\ 0 & 0 & 0 & a_1^2 & a_2^2 & a_3^2 & 0 & 0 & 0 \\ 0 & 0 & 0 & 0 & 0 & 0 & a_1^3 & a_2^3 & a_3^3 \end{bmatrix} \tag{18}$$

$$B = \begin{bmatrix} b_1^1 & b_2^1 & b_3^1 & 0 & 0 & 0 & 0 & 0 & 0 \\ 0 & 0 & 0 & b_1^2 & b_2^2 & b_3^2 & 0 & 0 & 0 \\ 0 & 0 & 0 & 0 & 0 & 0 & b_1^3 & b_2^3 & b_3^3 \end{bmatrix} \tag{19}$$

C. Identification of the CFR model

The identification task consists in estimating the coefficients of the matrices A and B according to equations (11). To achieve this aim, it is necessary to have available measured data of the CFR. Thus, the CFR is firstly modeled using the Saint-Venant equations via the software SIC [12]. A mean rectangular profile is considered with a bottom equal to $S = 52$ m, a length equal to $L = 42300\ m$ and a quasi-nul slope equal to $2.4e^{-5}$ %. Then, the actuators of the CFR are modeled using the software Matlab/Simulink. A simulation architecture coupling SIC and Matlab/Simulink allows the resolution of the Saint-Venant equations according to scenarios defined on Matlab/Simulink. These scenarios consist in the simulation of the operation of the locks and gates of the CFR.

The scenario, entitled "'scenario 1"', which is used for the identification of the matrices A and B corresponds to two days of navigation, with a positive discharge at Cuinchy equal to $0.6\ m^3/s$ and a discharge at Fontinettes equal to zero. The discharge at Aire-sur-la-Lys is considered such as a pulse signal with a frequency of $2.7e^{-4}\ Hz$ and a maximum amplitude of $2.6\ m^3/s$ from time 0 to 34 $hours$ and equal to zero thereafter (*see* Figure 3.a). It allows the water supply of the CFR to keep the level close to the NNL. During these two days, the increase of the CFR volume is due to 10 ships which have crossed the Cuinchy lock the first 10 hours and to the supplying flow of Aire-sur-la-Lys. The decrease of the CFR volume is due to the 20 ships crossing the Fontinettes lock. The simulation of the operating of the Cuinchy lock corresponds to a volume of $3700\ m^3$ during 6 minutes with a trapezoidal profile, and a maximum discharge equal to $10.8\ m^3/s$. The operation of the Cuinchy lock causes wave phenomena along the CFR with an amplitude maximum equal to 9 cm (*see* Figure 3.b). The wave is attenuated one day after the last Cuinchy lock operation. The simulation of the operating of the Fontinettes lock corresponds to a volume of $25000\ m^3$ during 15 minutes with a trapezoidal profile, and a maximum

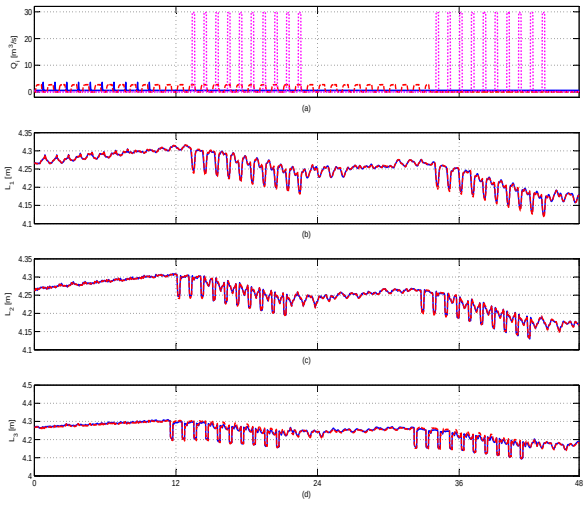

Figure 3. Scenario 1, (a) discharges at Cuinchy Q_1 (blue continuous line), at Aire-sur-la-Lys Q_2 (red dotted line) and at Fontinettes Q_3 (magenta dashed line), levels at (b) Cuinchy L_1, (c) Aire-sur-la-Lys L_2 and (d) Fontinettes L_3.

Table I
COEFFICIENTS OF THE MATRIX A ($\times e^{-1}$).

a_1^1	a_2^1	a_3^1	a_1^2	a_2^2	a_3^2	a_1^3	a_2^3	a_3^3
6.77	2.61	0.61	2.73	3.9	3.34	4.08	3.88	2.04

Table II
COEFFICIENTS OF THE MATRIX B ($\times e^{-3}$).

b_1^1	b_2^1	b_3^1	b_1^2	b_2^2	b_3^2	b_1^3	b_2^3	b_3^3
0.4	1.2	0.2	0.3	1	0.3	0.6	1.3	2.8

discharge equal to 29 m^3/s. The operation of the Fontinettes lock causes wave phenomena along the CFR with an amplitude maximum equal to 13 cm.

These signals obtained according to the SIC/MATLAB/Simulink architecture are used to identify the model of the CFR. Due to the properties of the signals, the matrix $(\overline{\Phi}\ \overline{\Phi}^T)$ of the equation (11) can be singular. Thus it is often necessary to use the Moore-Penrose pseudoinverse of this matrix. Finally, the coefficients of the matrices A and B are given by Tables I and II, respectively.

After the identification step, the outputs of the model $\hat{y}(k)$ and the measured levels $y(k)$ are compared as depicted in Figure 4. The estimated ouputs in red dashed line are very close to the measured levels in blue continuous line. To estimate the effectiveness of the model, a fitting indicator (FIT) is defined as $FIT = (1 - \frac{||\hat{y}-y||_2}{||y-y_m||_2}) \times 100$, where y_m is a column vector composed of the mean value of y. For this scenario, the FIT are given for each level in Table III.

The effectiveness of the CFR model has to be estimated on other scenarios. These tests are presented in the next section.

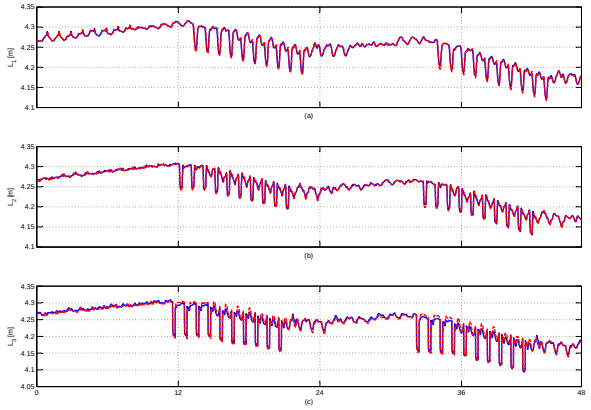

Figure 4. Scenario 1 - estimated (red dashed line) and measured (blue continuous line) levels at (a) Cuinchy L_1, (b) Aire-sur-la-Lys L_2 and (c) Fontinettes L_3.

Table III
FIT INDICATORS FOR THE "'SCENARIO 1"' (%).

FIT_{L_1}	FIT_{L_2}	FIT_{L_3}
93	93	87

IV. EVALUATION OF THE CFR STATE-SPACE MODEL

The evaluation of the effectiveness of the CFR model is carried out according to several scenarios as the crossing of one ship in Cuinchy, one ship in Fontinettes, twenty ships in Fontinettes, ten ships in Cuinchy and ten ships in Fontinettes the first day, etc. All these scenarios are not presented herein. The second presented scenario, entitled "'scenario 2"', consists in the simulation of the crossing of ten ships in Fontinettes (*see* Figure 5.a). The discharge on Cuinchy is equal to zero. On Aire-sur-la-Lys, the discharge corresponds to a pulse signal with a frequency of $2.7e^{-4}$ Hz and a maximum amplitude of 1.8 m^3/s. The outputs of the model $\hat{y}(k)$ and the measured levels $y(k)$ are compared as depicted in Figure 5.b-5.d for each level. They are close to the measured ones.

The third scenario, entitled "'scenario 3"', consists in the simulation of the crossing of ten ships in Cuinchy the first ten hours and ten ships in Fontinettes the last ten hours of the first day simulating the navigation of ten ships on the CFR (*see* Figure 6.a). The discharge on Cuinchy is equal to 0.6 m^3/s. On Aire-sur-la-Lys, the discharge corresponds to a pulse signal with a frequency of $2.7e^{-4}$ Hz and a maximum amplitude of 1.8 m^3/s. For each level, the outputs of the model $\hat{y}(k)$ and the measured levels $y(k)$ are compared as depicted in Figure 6.b-6.d.

In these two scenarios, the estimated outputs are close to the measured data, as shown the Figures 5 and 6. The FIT indicators (*see* Table IV) confirm the effectiveness of the CFR gray-box model on several scenarios.

V. CONCLUSION

Gray-box state-space modeling approach of an inland navigation reach is presented in this paper. It requires a good

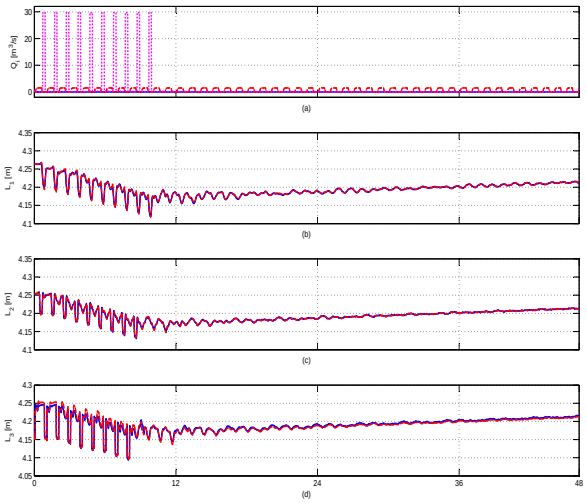

Figure 5. Scenario of Cuinchy lock and Fontinettes lock crossed each one by 10 ships - (a) Discharges in Cuinchy (blue continuous line), in Aire-sur-la-Lys (red dashed line) and in Fontinettes (magenta dotted line), and estimated (red dashed line) and measured (blue continuous line) levels at (b) Cuinchy L_1, (c) Aire-sur-la-Lys L_2 and (d) Fontinettes L_3.

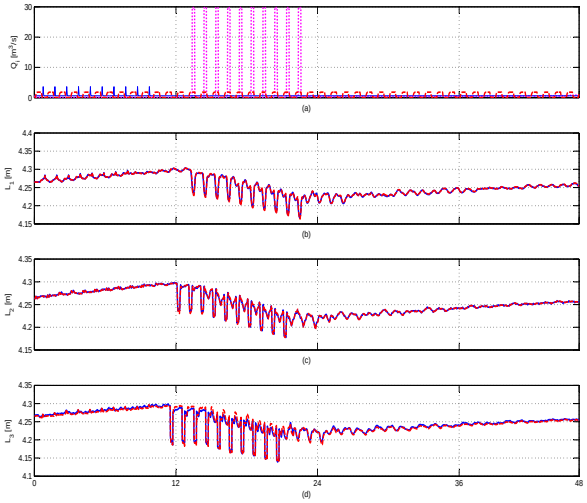

Figure 6. Scenario of Cuinchy and Fontinettes locks crossed by 10 ships - (a) Discharges in Cuinchy (blue continuous line), in Aire-sur-la-Lys (red dashed line) and in Fontinettes (magenta dotted line), and estimated (red dashed line) and measured (blue continuous line) levels at (b) Cuinchy L_1, (c) Aire-sur-la-Lys L_2 and (d) Fontinettes L_3.

Table IV
FIT INDICATORS FOR THE "'SCENARIO 2"' AND "'SCENARIO 3"' (%).

"'scenario 2"'			"'scenario 3"'		
FIT_{L_1}	FIT_{L_2}	FIT_{L_3}	FIT_{L_1}	FIT_{L_2}	FIT_{L_3}
92	92	84	90	89	79

estimation of the time-delays characterizing the dynamics of the open-channel system. This approach is used for the Cuinchy-Fontinettes reach located in the North of France. This reach is a large system equipped with locks and gates. It is impacted by wave phenomena due to the lock operations. The identification approach is performed according to data from a simulation architecture based on a software which allows the resolution of Saint-Venant equations. Then, the effectiveness of the identified model is evaluated by considering several scenarios.

The future purposes consist in testing the proposed modeling approach by considering unknown inputs and outputs which are often present in the real case, and in adapting this approach, if necessary, to improve the accuracy of the model. Then, this approach should be used to model the Cuinchy-Fontinettes reach with real data. The state-space model of the Cuinchy-Fontinettes reach will be used to design control algorithms to attenuate the wave phenomena. Moreover, this model will be used to conceive FDI techniques to improve the reliability of the Cuinchy-Fontinettes reach.

ACKNOWLEDGMENT

This work is a contribution to the GEPET'Eau project which is granted by the French ministery MEDDE - GICC, the French institution ORNERC and the DGITM.

REFERENCES

[1] J. Blesa, E. Duviella, M. Sayed-Mouchaweh, V. Puig and K. Chuquet, *Automatic control to improve the seaworthiness conditions in inland navigation networks: application to a channel in the north of France*, International conference on Maritime Transport, Barcelone, Espagne, 27-29 Juin 2012.

[2] C. Brand, M. Tran and J. Anable (2012). *The UK transport carbon model: An integrated life cycle approach to explore low carbon futures*, Energy Policy, Volume 41, February 2012, Pages 107-124.

[3] V. T. Chow, (1959). *Open-channel hydraulics*, McGraw-Hill. New York.

[4] Camacho, E. F. and Bordons, C. (2004). *Model Predictive Control*. Springer, Great Britain.

[5] Ten Broeke, I.A.A., C.P.M. Willems and C.C. Glansdorp (2001). A joint European effort to enhance safety and usability of the inland waterway network. In 2001 IEEE Intelligent Transportation Systems Conference Proceedings. Oakland (CA) USA August 2001.

[6] Fastenbauer, M.; M. Sattler and G. Schilk (2007). River Information Services for commercial users in the Inland Waterway sector. In proceedings International Symposium on Logistics and Industrial Informatics. Wildau, Germany. Setember 2007.

[7] O. Le Pocher, E. Duviella, L. Bako and K. Chuquet, *Sensor fault detection of a real undershot/overshot gate based on physical and nonlinear black-box models*, Safeprocess'12, Mexico, Mexique, 29-31 August 2012.

[8] X. Litrico and V. Fromion, *Simplified modeling of irrigation canals for controller design*. Journal of Irrigation and Drainage Engineering, Vol. 130, No. 5, pp. 373-383, 2004.

[9] X. Litrico and V. Fromion, *Modeling and Control of Hydrosystems*, Springer, 2009.

[10] Ljung, L. (1987). System identification: Theory for the user, Prentice-Hall. Englewood Cliffs, N.J.

[11] Maciejowski, J.M. (2002). Predictive Control: With Constraints. Prentice Hall, 2002.

[12] P. O. Malaterre, *SIC 5.20, Simulation of irrigation canals*, http://www.cemagref.net/sic/sicgb.htm, 2006.

[13] I. Mallidis, R. Dekker and D. Vlachos (2012). *The impact of greening on supply chain design and cost: a case for a developing region*, Journal of Transport Geography, Volume 22, May 2012, Pages 118-128.

[14] S. Mihic, M. Golusin and M. Mihajlovic (2011). *Policy and promotion of sustainable inland waterway transport in Europe - Danube River*, Renewable and Sustainable Energy Reviews, Volume 15, Issue 4, May 2011, Pages 1801-1809.

[15] K. Tan, Y. Li, P. Gawthrop and A. Glidle (1997). *Evolutionary Grey-Box modelling for Practical Systems*. Technical Report CSC-96019, Centre for Systems and Control, University of Glasgow.